

# Microstructure of ternary system di-lauroyl-phosphatidyl-adenosine/water/cyclohexane

Francesca Betti,<sup>a</sup> Francesca Baldelli Bombelli,<sup>a</sup> Debora Berti,<sup>a</sup> Massimo Bonini,<sup>a</sup>  
Astrid Brandt<sup>b</sup> and Piero Baglioni<sup>a\*</sup>

<sup>a</sup>Department of Chemistry and CSGI, University of Florence, Florence, Italy, and <sup>b</sup>Hahn Meitner Institute, Berlin, Germany. Correspondence e-mail: baglioni@csgi.unifi.it.

1,2-Dilauroyl-*sn*-glycero-3-phosphatidyl-adenosine in 0.1 M phosphate buffer (pH = 7.5) forms worm-like micelles that with ageing of the solution, self-assemble into helical superstructures. Small-angle neutron scattering has shown that dissolution of even small amounts of oil in the hydrophobic cores induces a dramatic structural transition to form spherical micelles. A variation of the interfacial film curvature promotes a strong change in base–base interaction pattern as shown in circular dichroism experiments.

© 2007 International Union of Crystallography  
Printed in Singapore – all rights reserved

## 1. Introduction

In nature, genetic information is stored and replicated by means of specific recognition processes displayed by the selective binding of nucleobases through hydrogen bonds and stacking interactions. The base pairing, otherwise unfavourable in aqueous media, is promoted by the macromolecular arrangement of nucleobases of the sugar–phosphate skeleton, responsible for the cooperative effect that leads to the coupling of two polynucleotide strands (Iwaura *et al.*, 2003; Yoshina-Ishii & Boxer, 2003; Scheidt *et al.*, 2004; Moreau *et al.*, 2004).

In the last decade, researchers have exploited nature *strategy*, *i.e.* DNA-based recognition patterns, in the design of new self-assembling structures formed by bio-inspired surfactants that represent an optimum starting point for the development of molecular devices for pharmaceutical and medical applications.

Phospholiponucleosides, whose self-assembling behaviour has been recently explored by our group (Berti *et al.*, 1999; Baglioni & Berti, 2003; Baldelli Bombelli *et al.*, 2004), are synthetic amphiphilic molecules composed of a phospholipid hydrophobic moiety and a nucleotidic polar head that reproduces the functionalities and the charge of DNA monomers.

The initial interest in such derivatives was boosted by their possible use as lipophilic nucleosidic analogue derivatives in myeloid leukaemia treatment (Shuto *et al.*, 1988). More recently, the use of AZT (3'-azido-3'-deoxythymidine, a modified nucleoside) in HIV therapy and the realisation that the *bare* nucleoside is inefficient in entering the blood-brain barrier sparked the use of *smart prodrugs*. Phosphatidyl nucleosides are chemically converted into nucleoside triphosphates which exert antiviral action by inhibiting the reverse transcriptase in a metabolic pathway carried on by phospholipase (Yatwin *et al.*, 1999).

We are interested in the expression of molecular functions, contained in the polar heads, displayed by phosphatidyl nucleoside self-assemblies, where the driving force for the aggregation is hydrophobic, *i.e.* the exclusion of hydrocarbon chains from contact with the aqueous medium. This effect is cooperative and various topologies, like globular, rigid or flexible cylindrical micelles, or bilayers can be formed as a result of packing preferences of the

constituting surfactant molecule. Indeed, short-chain derivatives, like 1,2-dioctanoyl-*sn*-glycero-3-phosphatidyl nucleosides, form quasi-spherical micelles (positive curvature), while long-chain derivatives, such as 1,2-dioleoyl-*sn*-glycero-3-phosphatidyl nucleosides (Berti *et al.*, 1999), organize into bilayer structures (lamellar phase and liposome) with zero curvature (Milani *et al.*, 2006).

Recently, we have focused our attention to the self-aggregation behaviour of 1,2 dilauroyl-*sn*-glycero-3-phosphatidyl nucleosides (DLP-Nucleosides), whose spontaneous interfacial curvature promotes the formation of cylindrical micelles in phosphate buffer (PBS). The size and the shape of the aggregates show a noticeable dependence on the nucleolipid concentration and on the nature of the polar head. In fact, while DLP-Uridine (DLPU) forms worm-like micelles which undergo an axial growth as surfactant concentration is increased and eventually entangle in a transient network (Baldelli Bombelli *et al.*, 2002; Baldelli Bombelli *et al.*, 2004), DLP-Adenosine (DLPA) cylindrical micelles evolve during ageing into helical suprastructures as a consequence of the higher stacking capacity (purine–purine > purine–pyrimidine > pyrimidine–pyrimidine) of adenosine with respect to uridine (Baldelli Bombelli *et al.*, 2006).

On this basis, we have investigated how surface curvature affects the interaction pattern at the interface by introducing a third component (cyclohexane) to the previously studied DLPA binary system, *i.e.* by changing the distance and the orientation of the nucleosidic groups at the interface. We have chosen the DLPA system because we are particularly interested in the effect of cyclohexane on the stacking and hydrogen bonding interactions that are more enhanced for this derivative.

In this paper, we report a microstructural characterization of DLPA micelles in 0.1 M PBS (pH = 7.5) and their evolution as oil volume fraction is increased, as revealed by small-angle neutron scattering (SANS) and circular dichroism (CD). SANS measurements have been performed at different contrast conditions using hydrogenated and deuterated cyclohexane in order to highlight different regions of the aggregates. This structural characterization is correlated with CD results, which give information on polar head environment upon cyclohexane addition.

## 2. Experimental section

### 2.1. Materials

1,2-Dilauroyl-*sn*-glycero-3-phosphocholine (DLPC) was purchased from Avanti Polar Lipids (Alabaster, Alabama, USA) and its purity checked by TLC. The lecithin was used as received since no oxidation or lyso products could be detected. Adenosine, HCl, CHCl<sub>3</sub>, MeOH and NH<sub>3</sub> (33% aqueous solution) used in the synthesis and NaH<sub>2</sub>PO<sub>4</sub> (>>99%) and Na<sub>2</sub>HPO<sub>4</sub> (>>99%), were purchased from Fluka (Switzerland). Phospholipase D from *Streptomyces* sp AA586 was a generous gift from Asahi Chemical Industry Co., Ltd (Tokyo, Japan). Deuterium oxide (>99.5%) and deuterated cyclohexane (>99.7%) for SANS measurements was provided by Euriso-Top, (Saclay, Gif-sur-Yvette, France). Hydrogenated cyclohexane was purchased from Fluka. DLPA was synthesized starting from the corresponding phosphatidylcholine in a two-phase system according to a modification of the method proposed by Shuto and coworkers (Shuto *et al.*, 1988) and obtained as an ammonium salt. Molecular structure is reported in Fig. 1. The lyophilized powder was dissolved in 0.1 M phosphate buffer (PBS) at pH = 7.5 prepared in water (for CD) or in deuterated water (for SANS), in order to obtain a concentration of  $2 \times 10^{-2}$  M, corresponding to a surfactant volume fraction  $\phi_{\text{surf}}$  of  $1.2 \times 10^{-2}$ . We have also prepared ternary systems at the same  $\phi_{\text{surf}}$  with different amounts of deuterated or hydrogenated cyclohexane:  $\phi_{\text{oil}}(v/v)$  0.003 and 0.008. All the samples are in the region of the microemulsion phase diagram below the emulsification failure ( $\phi_{\text{oil}} \approx 0.01$ ), *i.e.* there is no excess oil phase.

### 2.2. Small-angle neutron scattering

Small-angle neutron scattering experiments were performed on the V4 spectrometer (BENSCH-Hahn Meitner Institut-Berlin). Three different configurations (*i.e.* sample-detector distances: 1 m, 4 m and 16 m) allowed to cover a range of scattering vector magnitudes  $q = (4\pi/\lambda)\sin(\theta/2)$   $3.8 \times 10^{-3} \text{ \AA}^{-1}$ – $0.3 \text{ \AA}^{-1}$  with  $6.1 \text{ \AA}$  neutrons and a wavelength spread  $\Delta\lambda/\lambda \approx 10\%$ . 0.1 M deuterated phosphate buffer (D-PBS) at pH = 7.5 was chosen as a solvent in order to enhance the scattering contrast and minimize the incoherent background from hydrogen. Data reduction has been accomplished according to the standard BENSCH procedure (Keiderling, 1994) for small-angle isotropic scattering. All experiments were performed at the temperature of  $298 \pm 0.1$  K.

**2.2.1. SANS data analysis.** In this study the complete determination of PBS/DLPA/cyclohexane microemulsion structure has been obtained by using two contrast profiles differing for the isotopic composition of cyclohexane: ‘CORE’ profile for the system D-PBS/DLPA/C<sub>6</sub>H<sub>12</sub> and ‘SHELL’ profile for the system D-PBS/DLPA/C<sub>6</sub>D<sub>12</sub>. The terms ‘CORE’ and ‘SHELL’ correspond to the portion of the micelle highlighted by each contrast condition. In the ternary system D-PBS/DLPA/C<sub>6</sub>H<sub>12</sub>, the term ‘CORE’ is used to indicate the

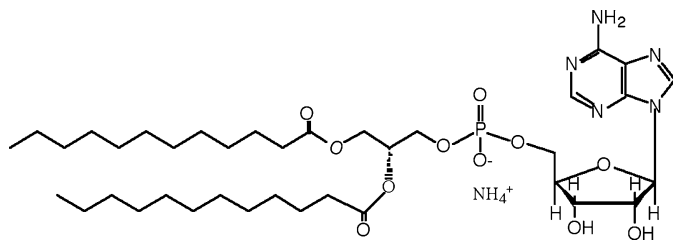


**Figure 1**  
Schematic drawing of the chemical structure of DLPA.

**Table 1**

Scattering length densities used in the analysis of SANS data.

	SLD ( $\times 10^{-6} \text{ \AA}^{-2}$ )
D <sub>2</sub> O	6.36
C <sub>6</sub> H <sub>12</sub>	−0.28
C <sub>6</sub> D <sub>12</sub>	6.70
DLPA	1.55
Polar head	4.19
Tail+oil	−0.37

region occupied by the hydrocarbon tails and the oil, whose scattering length densities (SLDs) are very similar and, at the same time, smaller than the ones of the polar heads and D<sub>2</sub>O. When both solvents, water and cyclohexane, are deuterated, the ‘SHELL’ seen by neutrons is the surfactant film: in fact in this case the two solvents have comparable SLD and are very different from the DLPA one. On the basis of this ‘CORE–SHELL’ contrast model we can define the different aggregate moieties as  $R_{\text{apolar}}$ , which is the radius of the oil core plus surfactant tail,  $\delta_{\text{h}}$  the polar head,  $R_{\text{oil}}$  the radius of cyclohexane core and  $\delta_{\text{s}}$  the overall surfactant length.

The analysis of SANS experimental data was performed using the routines provided by the SANS group at NIST Center for the Neutron Research (Gaithersburg, USA). Since these routines are not designed to reproduce more than one form factor at once, they were modified in order to simulate a mixed system constituted by spherical and cylindrical micelles. Due to the dilution of the system, inter-aggregate interactions have been considered negligible. Spherical micelles have been modelled as polydisperse cores with a shell of constant thickness (Bartlett & Ottewill, 1992), for cylindrical objects, a form factor of monodisperse (in the cross-section) cylinders with a core-shell SLD profile was used. The SLD of the different regions of the aggregates was evaluated from the atomic scattering lengths (Table 1) and the respective molecular volumes, and kept constant during the fitting. The total volume fractions are known and equal to the sum of the surfactant and the oil volume fractions.

The variable parameters were: the volume fraction for the mixed systems, the core radii  $R_{\text{apolar}}$  and  $R_{\text{oil}}$ , the polydispersity of the core according to a Schulz distribution  $\sigma_{\text{core}}$  (Schulz, 1939), and the shell thickness  $\delta_{\text{s}}$  and  $\delta_{\text{h}}$ . The investigated  $q$ -range is not extended enough to infer a quantitative evaluation of the cylinder contour length.

The structural parameters  $R_{\text{apolar}}$ ,  $R_{\text{oil}}$ ,  $\delta_{\text{s}}$  and  $\delta_{\text{h}}$  were obtained from the simultaneous fitting of the ‘CORE’ and the ‘SHELL’ corresponding samples in order to get a global minimization that accomplishes both the profiles. Moreover, the polar head thickness,  $\delta_{\text{h}}$ , that is the same for spherical and cylindrical micelles, is extracted from the binary PBS/DLPA system and just optimized during the fitting procedure (Baldelli Bombelli *et al.*, 2004).

### 2.3. Circular dichroism

CD spectra have been collected on a J-715 Jasco spectropolarimeter. Samples were inserted into Hellma quartz cylindrical cells, whose path length was selected so that the samples did not exceed 0.8 optical density. The observed circular dichroism is then converted into molar ellipticity that is normalized for path length and dichroic chromophore concentration.

## 3. Results and discussion

The binary system H(D)-PBS/DLPA has been studied through cryo transmission electron microscopy (Cryo-TEM), dynamic light scattering, <sup>1</sup>H NMR and CD. Freshly prepared solutions are mostly

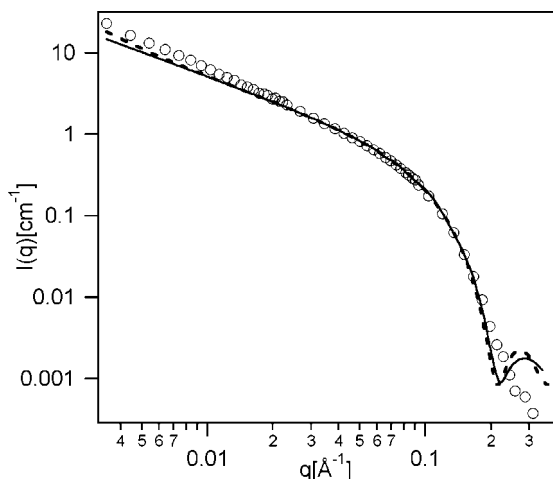


**Figure 2**  
SANS spectrum of a 4 d annealed  $2 \times 10^{-2} M$  DLPA sample in D-PBS 0.1 M at pH = 7.5 (open circles are experimental points) fitted with a core-shell cylindrical form factor (solid line) and flexible cylindrical form factor (dotted line).

composed of thread-like micelles whose cross-section, about 5 nm, is invariant with surfactant concentration while the axial dimension grows as a function of the lipid volume fraction. Cryo-TEM shows that DLPA threadlike micelles are not stable structures; in fact, annealed samples form giant helical superstructures composed by several single filaments joined together. The phase evolution to form helical superstructures occurs at the expenses of smaller threadlike micelles that are still present in the annealed samples. After 4 d the system does not evolve anymore; furthermore CD and  $^1H$  NMR findings proved that stacking interactions and hydrogen bonds among nucleic bases drive the self-assembling process to helical aggregates (Baldelli Bombelli *et al.*, 2006).

In Fig. 2 we report the SANS spectrum of  $2 \times 10^{-2} M$  DLPA in D-PBS after 4 d from preparation. The logarithmic plot highlights a scaling behaviour, which is a  $q^{-\alpha}$  scattering law, generally considered a fingerprint of the dimensionality of the aggregate in this momentum transfer range. The absence of a ‘pure’  $q^{-1}$  law in the intermediate-low  $q$  region (found for DLPU) (Baldelli Bombelli *et al.*, 2002; Baldelli Bombelli *et al.*, 2004) that is the fingerprint of cylindrical aggregates demonstrates a more complex self-assembling behaviour.

The scaling exponent of scattering law is about 1.2, not ascribable to a characteristic aggregate dimensionality or shape, that might derive from different and overlapping scaling behaviours, due to the coexistence of several shapes characterized by different local curvatures (worm-like micelles and giant helical suprastructures). To further prove this point, a fit of experimental data with both a core-shell cylinder form factor and a flexible cylinder form factor (Baldelli Bombelli *et al.*, 2004) highlights major deviations in the intermediate-low  $q$  region and confirms our hypothesis. For  $q > 0.025 \text{ \AA}^{-1}$  the agreement is instead good; hence we can extract a cylinder radius cross-section of about 21 Å, which is reasonable for DLPA worm-like micelles (Baldelli Bombelli *et al.*, 2006).

The cyclohexane addition to DLPA micellar solutions affects the average curvature of the aggregates, therefore modulating the base-base interaction pattern. SANS spectra of both ternary systems D-PBS/DLPA/ $C_6H_{12}$  and D-PBS/DLPA/ $C_6D_{12}$  at  $\phi_{oil}$  of 0.003 and 0.008 are reported in Fig. 3.

The spectra indicate a pronounced dependence of the micellar structure on cyclohexane volume fraction. Major differences are observed in the low-intermediate  $q$  region where a different scaling behaviour,  $q^{-\alpha}$ , indicates a different local structure of the aggregates. The spectra at low oil volume fraction (0.003) display a logarithmic decay ( $\alpha \simeq 1$ ) indicative of cylindrical micelles, while the spectra at high  $\phi_{oil}$  (close to the emulsification failure,  $\phi_{oil} \simeq 0.01$ ) have an  $\alpha$  value very close to zero, pointing out that a Guinier plateau is reached. In this case the radius of gyration of the aggregate,  $R_g$ , can be evaluated through asymptotic Guinier law for  $q \cdot R_g < 1$ . Assuming a spherical shape for the aggregates, we can evaluate  $R_g$  from  $R_g = \sqrt{3/5}R$ . Most likely these spherical micelles are polydisperse; the size distribution and its width can be determined through a model fitting, in this way an average  $R_g$  can be evaluated, as we will show later on.

For the samples at low  $\phi_{oil}$ , a qualitative estimation of the cylinder cross-section can be determined through a modified Guinier plot in the intermediate  $q$ -region,  $\ln[I(q) \cdot q]$  versus  $q^2$ , being valid the following expression (Lin *et al.*, 1987)

$$\ln[I(q) \cdot q] = \ln \left[ (c - c_{cmc}) \left( \frac{\pi N}{L} \right) (b_m - \rho_s v_m)^2 \right] - \frac{R_g^2 q^2}{2}, \quad (1)$$

where  $N$  is the aggregation number,  $L$  is the length of cylinder,  $b_m$  is the scattering length of aggregate,  $\rho_s$  is the SLD of the solvent,  $v_m$  is the volume of the aggregates and  $R_g$  is the radius of gyration of the

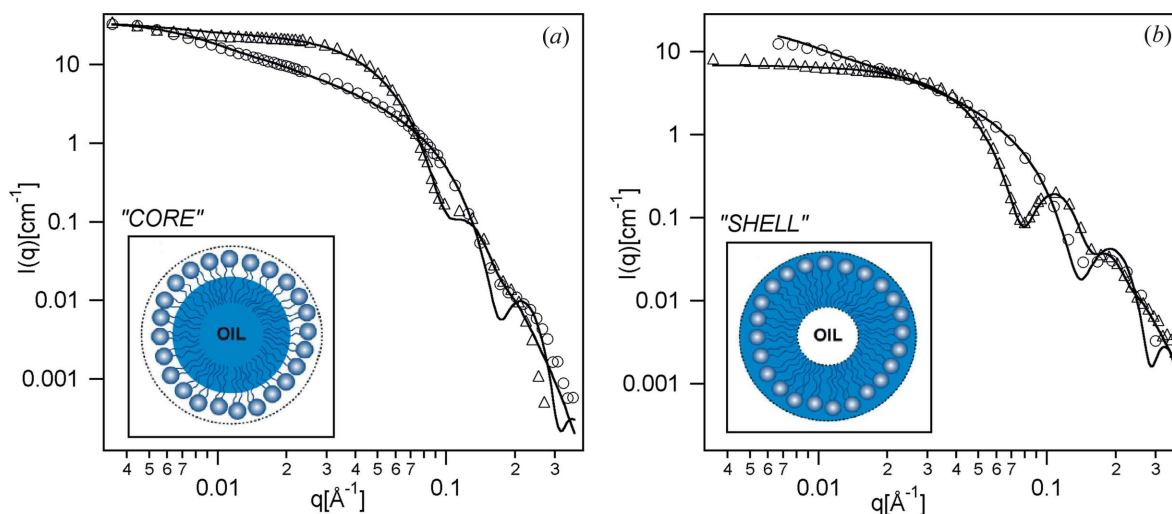


**Figure 3**  
SANS spectra of the ternary system D-PBS/DLPA/cyclohexane with hydrogenated (a) and with deuterated (b) cyclohexane, respectively. (open circles)  $\phi_{oil} = 0.003$  and (open triangles)  $\phi_{oil} = 0.008$ . The solid lines are the fitting curves; details are reported in the text. Inset: schematic representation of the contrast profiles used.

cross-sectional area of the cylinder (for uniform rod-like structures  $R_c = R/\sqrt{2}$ ). The evaluated values for  $R_c$  are reported in Table 2 as  $R^{**}$  and represent different moieties of the aggregate according to the contrast profile used. These values are in good agreement with the structural parameters extracted through the model fitting as showed below in the text.

To get some information on a more quantitative basis, a model fitting is necessary. However, it is not possible to fit the low  $\phi_{oil}$  spectra with a pure core-shell cylinder form factor, and, on the basis of Safran work on ‘fluctuating interfaces’ in microemulsions (Safran, 1992), where the simultaneous presence of two different structures is predicted, a coexistence of spheres and cylinders has been supposed. Therefore, a model obtained combining sphere and cylinder form factors was used for the data analysis (for details see the section on the SANS data analysis). The curve fittings are reported as solid lines in Fig. 3 and the resulting parameters are listed in Table 2.

The total cross-section radius ( $R_{apolar} + \delta_h$  for ‘CORE’,  $R_{oil} + \delta_s$  for ‘SHELL’) of the cylinder population is about 7 Å larger than the one obtained for the binary system, hence the introduction of a small amount of oil induces a swelling of the cylindrical aggregates and also the formation of a spherical micellar phase (20% of the total volume fraction) whose radius is nearly the same of the cylinder cross-section. Therefore, the initial swelling of the hydrophobic core of the aggregates already promotes dramatic change in the curvature of the lipid film sufficient to drive a structural transition.

Menge *et al.*, in a ternary system of nonionic surfactants, have found a similar behaviour but the cylinder-sphere transition occurred at higher oil volume fractions and no coexistence of the two phases has been observed (Menge *et al.*, 2003). This fact and the observation that no helical superstructures are detected by SANS (conventional  $q^{-1}$  scaling) indicate that interfacial curvature is the result of an extremely delicate balance, which is altered even by tiny variations in system composition.

Increasing the oil volume fraction close to the emulsification failure the cylinder-sphere transition occurs and the droplet size increases of about 20 Å; obviously the swelling concerns the hydrophobic region, *i.e.*  $R_{oil}$  and  $R_{apolar}$ .

The structural parameters are reported in Table 2. The radius of gyration determined by Guinier asymptotic law, once corrected for the polydispersity index, obtained through a Schulz distribution, is in good agreement with the model fitting value, as reported in Table 2.

**Table 2**

Structural parameters extracted by model fitting: total volume fraction,  $\phi_{TOT}$ , core radius (Å),  $R_{apolar}$  and  $R_{oil}$ , shell thickness (Å),  $\delta_h$  and  $\delta_s$ , and polydispersity  $\sigma_{core}$ .

D-PBS/DLPA/C <sub>6</sub> H <sub>12</sub>					
$\phi_{oil}$ (v/v)	$\phi_{TOT}^\dagger$	$R_{apolar}$	$\delta_h$	$\sigma_{core}$	$R^{**\ddagger}$
0.003	c 0.012	20.6	7.1	–	24.4
	s 0.003	19.3	7.1	0.187	
0.008	s 0.019	40.0	7.1	0.157	41.9

D-PBS/DLPA/C <sub>6</sub> D <sub>12</sub>					
$\phi_{oil}$ (v/v)	$\phi_{TOT}^\dagger$	$R_{oil}$	$\delta_s$	$\sigma_{core}$	$R^{**\ddagger}$
0.003	c 0.011	11.9	14.3	–	13.2
	s 0.005	11.5	14.3	0.187	
0.008	s 0.019	31.7	14.3	0.157	29.0

† c is cylinder and s is sphere. ‡ Data obtained from qualitative model-free analysis.

It might be interesting, to confirm through complementary techniques that structural changes are accompanied by a variation in base-base pattern.

CD is ideally suited for this purpose. In Fig. 4 we compared spectra of the binary and ternary system H-PBS/DLPA/C<sub>6</sub>H<sub>12</sub> at  $\phi_{oil} = 0.003$  and  $\phi_{oil} = 0.008$ . The consistent variation of molar ellipticities is indicative that the base environment at the interface is modulated by oil addition. Moreover, the slight change of minimum position, ascribed to the electronic transition  $\pi-\pi^*$ , with oil dissolution into the hydrophobic core, indicates a conformational variation at the film interface, where the chromophores are located. Interestingly the highest oil content CD spectrum is almost coincident with the one obtained for 1,2-dioctanoyl-*sn*-glycero-3-phosphatidyl-adenosine (diC<sub>8</sub>PA) (surfactant that differs from DLPA only in the tail length), globular micelles (Berti *et al.*, 2006) pointing out that the key factor is the interface curvature.

**4. Conclusions**

DLPA forms in 0.1 M PBS (pH = 7.5) worm-like micelles that, with the ageing of the solutions, assemble into helical superstructures. A subtle balance between base-base interactions at the interface and surfactant packing preferences determines the DLPA self-assembling

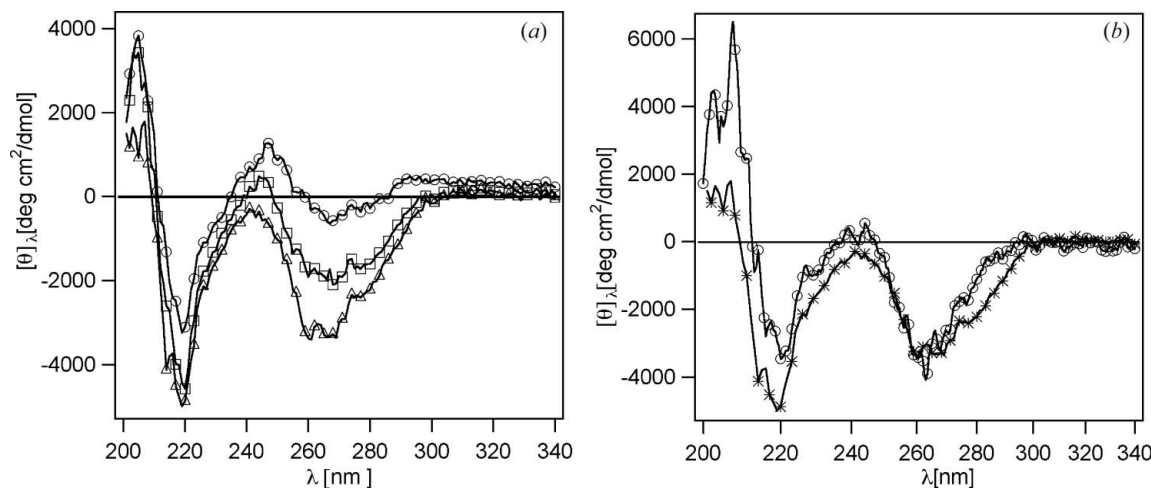


**Figure 4** (a) CD spectra of the ternary system H-PBS/DLPA/C<sub>6</sub>H<sub>12</sub> as a function of  $\phi_{oil}$ . (open squares)  $\phi_{oil} = 0\%$ , (open circles)  $\phi_{oil} = 0.003$  and (open triangles)  $\phi_{oil} = 0.008$ . (b) Comparison between CD spectra of diC<sub>8</sub>PA  $1 \times 10^{-2}M$  in H-PBS 0.1 M pH = 7.5 (stars) and H-PBS/DLPA/C<sub>6</sub>H<sub>12</sub> system at  $\phi_{oil} = 0.008$  (open circles).

behaviour. Small amounts of cyclohexane ( $\phi_{\text{oil}} = 0.003$  and  $0.008$ ) promote dramatic changes in the curvature of the lipid film sufficient to drive a structural transition: in fact, SANS experiments with internal contrast variation have shown already that the initial swelling of the hydrophobic core of the aggregates ( $\phi_{\text{oil}} = 0.003$ ) alters the interfacial curvature inducing the breaking of helical assemblies with the formation of cylindrical and spherical micelles. For  $\phi_{\text{oil}} = 0.008$  only a spherical micellar phase has been detected. These observations indicate that interfacial curvature is the result of an extremely delicate balance, which is modified even by tiny variations in system composition. CD results have confirmed that the base environment at the interface is modulated by oil addition.

The authors would like to acknowledge financial support from CSGI and Italian MIUR. The experiments at BENS in Berlin were supported by the European Commission under the 'Access to Research Infrastructures action of the Human Potential Programme (RII3-CT-2003-505925)'.

### References

- Baglioni, P. & Berti, D. (2003). *Curr. Opin. Colloid Interface Sci.* **8**, 55–61.
- Baldelli Bombelli, F., Berti, D., Almgren, M., Karlsson, G. & Baglioni, P. (2006). *J. Phys. Chem. B*, **110**, 17627–17637.
- Baldelli Bombelli, F., Berti, D., Keiderling, U. & Baglioni, P. (2002). *J. Phys. Chem. B*, **106**, 11613–11621.
- Baldelli Bombelli, F., Berti, D., Pini, F., Keiderling, U. & Baglioni, P. (2004). *J. Phys. Chem. B*, **108**, 16427–16434.
- Bartlett, P. & Ottewill, R. H. (1992). *J. Chem. Phys.* **96**, 3306–3318.
- Berti, D., Baldelli Bombelli, F., Fortini, M. & Baglioni, P. (2007). *J. Phys. Chem. B*. Submitted.
- Berti, D., Barbaro, P. L., Bucci, I. & Baglioni, P. (1999). *J. Phys. Chem. B*, **103**, 4916–4922.
- Iwaura, R., Yoshida, K., Masuda, M., Ohnishi-Kameyama, M., Yoshida, M. & Shimizu, T. (2003). *Angew. Chem. Int. Ed.* **42**, 1009–1012.
- Keiderling, U. (1994). *BerSANS Data reduction manual*. Berlin: HMI.
- Lin, T., Chen, S., Gabriel, N. E. & Roberts, M. F. (1987). *J. Phys. Chem.* **91**, 406–413.
- Menge, U., Lang, P. & Findenegg, G. H. (2003). *J. Phys. Chem. B*, **107**, 1316–1320.
- Milani, S., Baldelli Bombelli, F., Berti, D., Hauss, T., Dante, S. & Baglioni, P. (2006). *Biophys. J.* **90**, 1260–1269.
- Moreau, L., Barthélémy, P., El Maataoui, M. & Grinstaff, M. W. (2004). *J. Am. Chem. Soc.* **126**, 7533–7539.
- Safran, S. A. (1992). *Structure and Dynamics of Strongly Interacting Colloids and Supramolecular Aggregates in Solution*. Dordrecht: Kluwer Academic Publishers.
- Scheidt, H. A., Flasche, W., Cismas, C., Rost, M., Herrmann, A., Liebscher, J. & Huster D. (2004). *J. Phys. Chem. B*, **108**, 16279–16287.
- Schulz, G. V. Z. (1939). *Phys. Chem. Abt. B*, **43**, 25.
- Shuto, S., Ueda, S., Imamura, S., Fukukawa, K., Tsujino, M., Matsuda, A. & Ueda, T. (1988). *Chem. Pharm. Bull.* **36**, 209.
- Yatwin, M. B., Li, W., Meredith, M. J. & Shenoy, M. A. (1999). *Adv. Drug Deliv. Rev.* **39**, 165.
- Yoshina-Ishii, C. & Boxer, S. G. (2003). *J. Am. Chem. Soc.* **125**, 3696–3697.